



**HAL**  
open science

## **IL-7 receptor expression is frequent in T-cell acute lymphoblastic leukemia and predicts sensitivity to JAK inhibition**

Lucien Courtois, Aurélie Cabannes-Hamy, Rathana Kim, Marine Delecourt, Antoine Pinton, Guillaume Charbonnier, Mélanie Feroul, Charlotte L. Smith, Giulia Tueur, Cécile Pivert, et al.

► **To cite this version:**

Lucien Courtois, Aurélie Cabannes-Hamy, Rathana Kim, Marine Delecourt, Antoine Pinton, et al.. IL-7 receptor expression is frequent in T-cell acute lymphoblastic leukemia and predicts sensitivity to JAK inhibition. *Blood*, 2023, 142 (2), pp.158-171. 10.1182/blood.2022017948 . hal-04191646

**HAL Id: hal-04191646**

**<https://hal.science/hal-04191646v1>**

Submitted on 12 Jan 2024

**HAL** is a multi-disciplinary open access archive for the deposit and dissemination of scientific research documents, whether they are published or not. The documents may come from teaching and research institutions in France or abroad, or from public or private research centers.

L'archive ouverte pluridisciplinaire **HAL**, est destinée au dépôt et à la diffusion de documents scientifiques de niveau recherche, publiés ou non, émanant des établissements d'enseignement et de recherche français ou étrangers, des laboratoires publics ou privés.

## **IL7-receptor expression is frequent in T-cell acute lymphoblastic leukemia and predicts sensitivity to JAK-inhibition**

Tracking no: BLD-2022-017948R3

Lucien Courtois (Institut Necker Enfants-Malades, INSERM U1151, France) Aurelie CABANNES-HAMY (Centre Hospitalier de Versailles, France) Rathana Kim (Université Paris Cité - Hopital Saint-Louis APHP - INSERM U944, France) marine delecourt (APHP Hopital Necker Enfants Malades, France) Antoine Pinton (Institut Necker Enfants-Malades, INSERM U1151, France) Guillaume Charbonnier (Hopital Necker Enfants-Malades, France) Mélanie Féroul (Laboratory of Onco-Hematology, Assistance Publique-Hôpitaux de Paris (AP-HP), Hôpital Necker Enfants-Malades, France) Charlotte Smith (Institut Necker Enfants Malades, France) Giulia Tueur (Hôpital Necker Enfants-Malades, Laboratoire d'Onco-Hématologie, Assistance Publique-Hôpitaux de Paris (AP-HP), France) Cecile Pivert (Hôpital Necker Enfants-Malades, Laboratoire d'Onco-Hématologie, Assistance Publique-Hôpitaux de Paris (AP-HP), France) Estelle Balducci (Hôpital Necker-Enfants Malades, APHP, France) Mathieu Simonin (Institut Necker Enfants-Malades, INSERM U1151, France) laure hélène Angel (Assistance Publique-Hôpitaux de Paris (AP-HP), Hôpital Necker Enfants-Malades, Paris, France, France) Salvatore Spicuglia (Inserm, France) Nicolas Boissel (Hopital Saint-Louis, AP-HP, France) Guillaume Andrieu (Institut Necker Enfants-Malades, INSERM U1151, France) Vahid Asnafi (Hôpital Necker Enfants-Malades, Laboratoire d'Onco-Hématologie, Assistance Publique-Hôpitaux de Paris (AP-HP), France) Philippe Rousselot (Centre Hospitalier de Versailles, France) Ludovic Lhermitte (Hôpital Necker Enfants-Malades, Laboratoire d'Onco-Hématologie, Assistance Publique-Hôpitaux de Paris (AP-HP), France)

### **Abstract:**

T-cell acute lymphoblastic leukemia (T-ALL) is an aggressive hematological malignancy with a dismal prognosis related to refractory/relapsing diseases, raising the need for new targeted-therapies. Activating mutations of the IL7-receptor pathway genes (IL7Rp) play a proven leukemia-supportive role in T-ALL. JAK-inhibitors such as ruxolitinib have recently demonstrated preclinical efficacy. However, prediction markers for sensitivity to JAK-inhibitors are still lacking. Herein, we show that IL7R (CD127) expression is more frequent (~70%) than IL7Rp-mutations in T-ALL (~30%). We compared the so-called non-expressers (no IL7R-expression/IL7Rp-mutation), expressers (IL7R-expression without IL7Rp-mutation) and mutants (IL7Rp-mutations). Integrative multi-omics analysis outlined IL7R-deregulation in virtually all T-ALL subtypes, at the epigenetic-level in non-expressers, genetic-level in mutants, and post-transcriptional level in expressers. Ex-vivo data using primary-derived xenografts support that IL7Rp is functional whenever the IL7R is expressed, regardless of the IL7Rp mutational status. Consequently, ruxolitinib impaired T-ALL survival in both expressers and mutants. Interestingly, we show that expressers displayed ectopic IL7R-expression and IL7Rp-addiction conferring a deeper sensitivity to ruxolitinib. Conversely, mutants were more sensitive to venetoclax than expressers. Overall, combination of ruxolitinib and venetoclax resulted in synergistic effects in both groups. We illustrate the clinical relevance of this association by reporting achievement of complete remission in two patients with refractory/relapsed-T-ALL. This provides proof of concept for translation of this strategy into clinics as bridge to transplant. Altogether, IL7R-expression can be used as a biomarker for sensitivity to JAK-inhibition, thereby expanding the fraction of T-ALL patients eligible to ruxolitinib up to nearly ~70% of T-ALL.

**Conflict of interest:** No COI declared

**COI notes:**

**Preprint server:** No;

**Author contributions and disclosures:** All authors generated the data. LL, LC, RK, MD and VA collected, analyzed and managed the data. LL, LC and RK wrote the manuscript. GC, GA and AP performed bioinformatic analyses. NB, ACH and PR provided clinical data. LL designed the concept of the work and supervised analyses and writing.

**Non-author contributions and disclosures:** No;

**Agreement to Share Publication-Related Data and Data Sharing Statement:** Accession numbers: Study : EGAS00001007144 (<https://ega-archive.org/studies/EGAS00001007144>) Dataset : EGAD00001010273

**Clinical trial registration information (if any):**

**Figure 1. Landscape of IL7R expression in normal and malignant thymocytes**

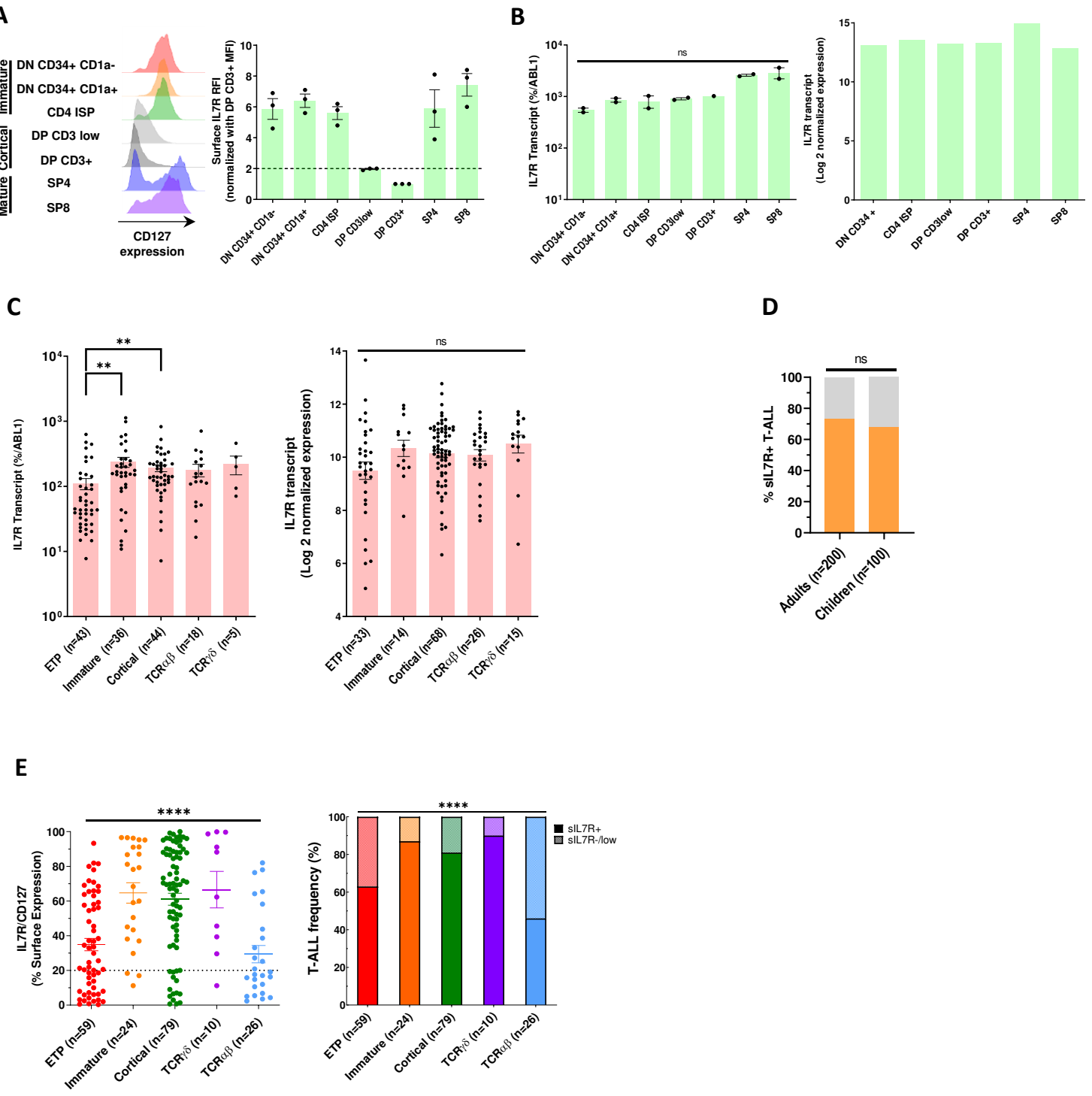
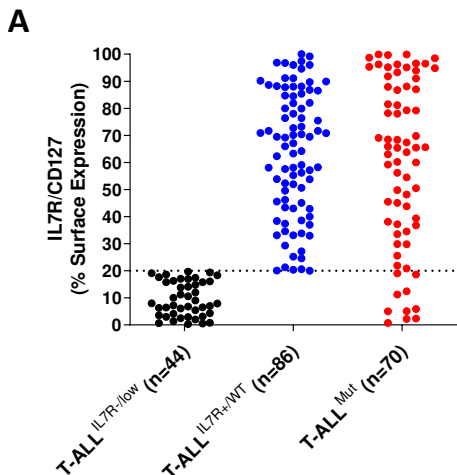
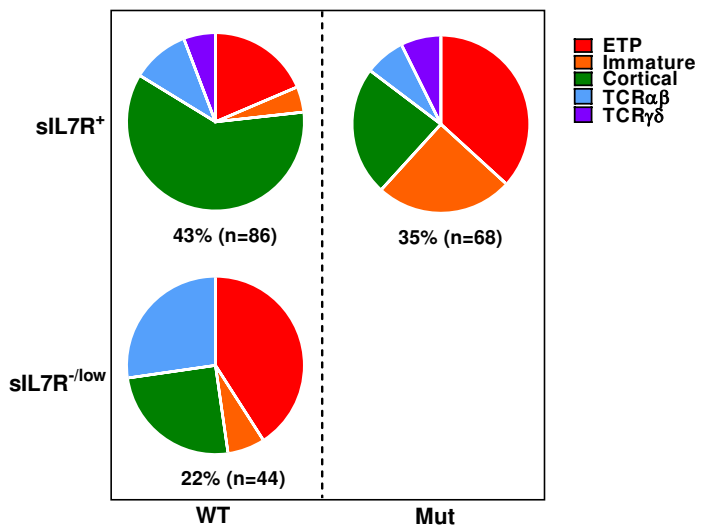
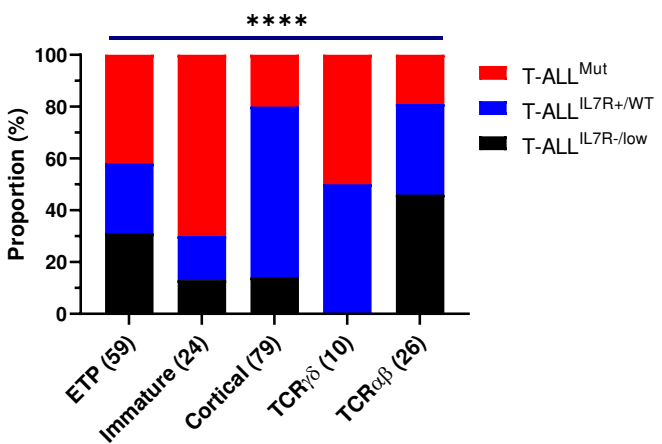


**Figure 2. CD127 expression and IL7R $\mu$  mutational status define 3 categories of T-ALL**



**B**



**C**

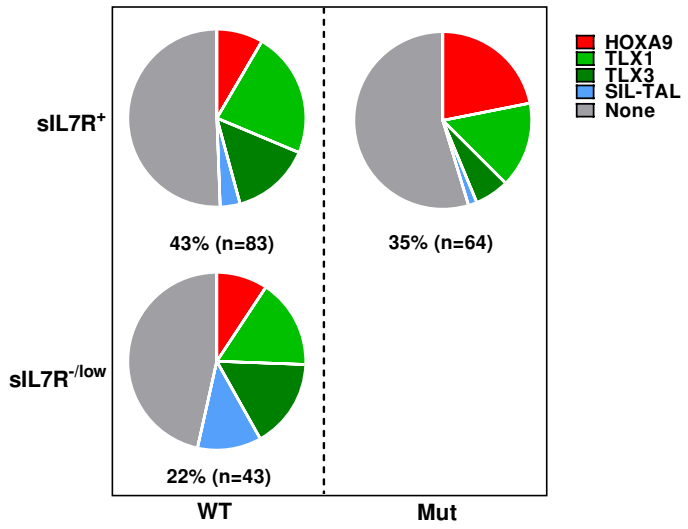
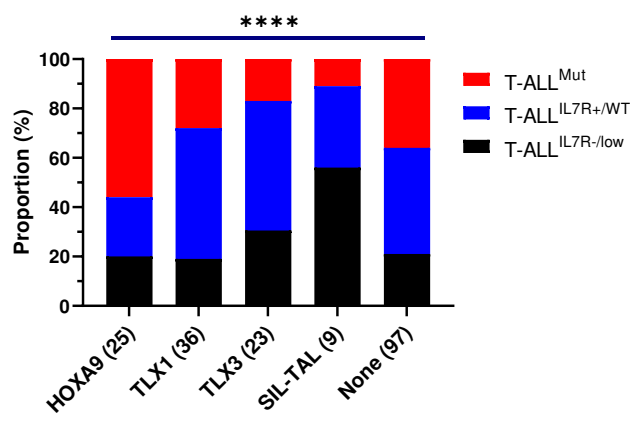


**Figure 3. Functional signaling and targeting of IL7R $\beta$  in normal and malignant thymocytes**

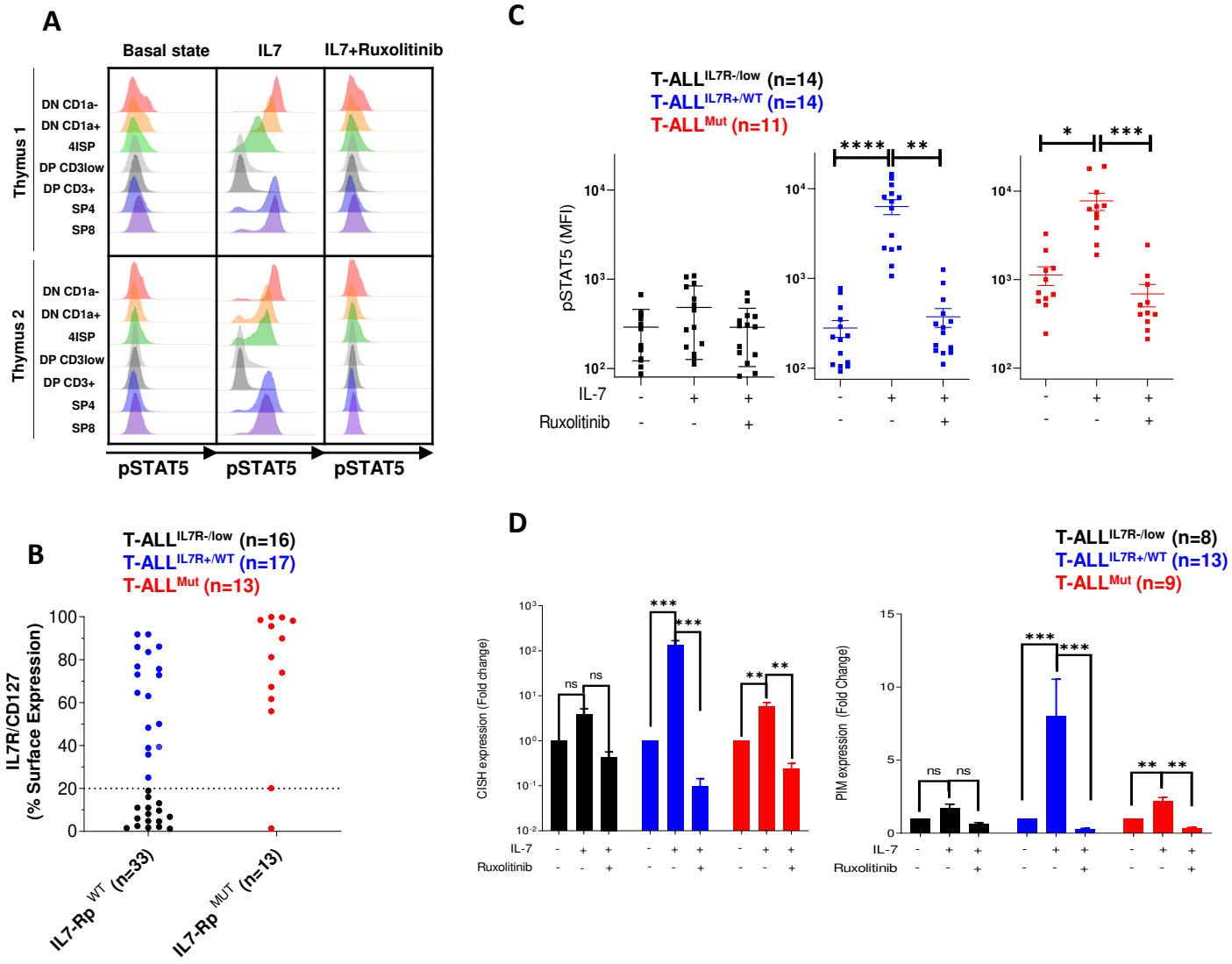


**Figure 4. Ruxolitinib induces apoptosis and cytostatic effects in IL7R+ T-ALL, irrespective of the IL7R pathway mutational status**

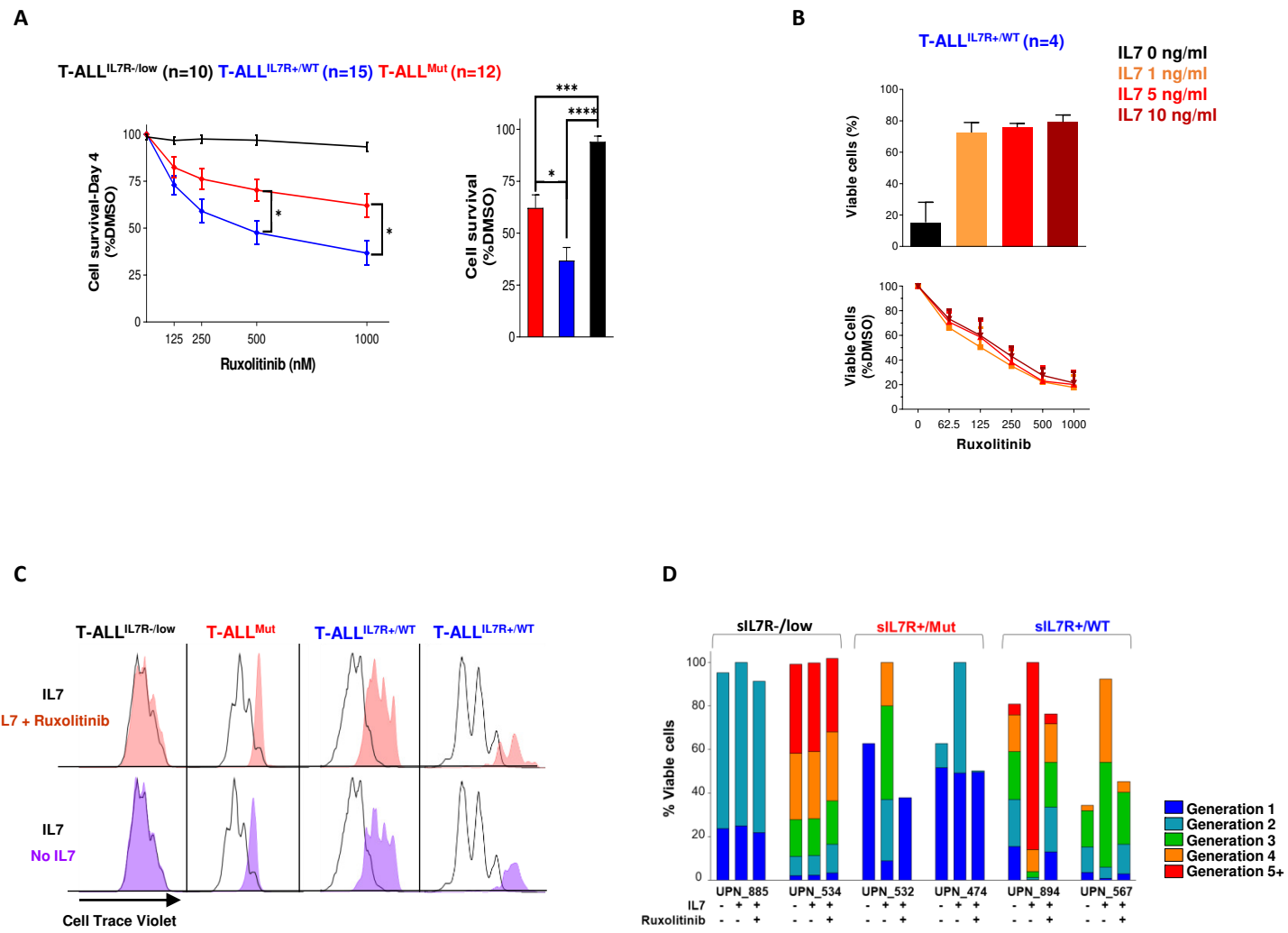


**Figure 5. Expressers highly sensitive to ruxolitinib are characterized by broad H3K4me3 domains on IL7R promoter**

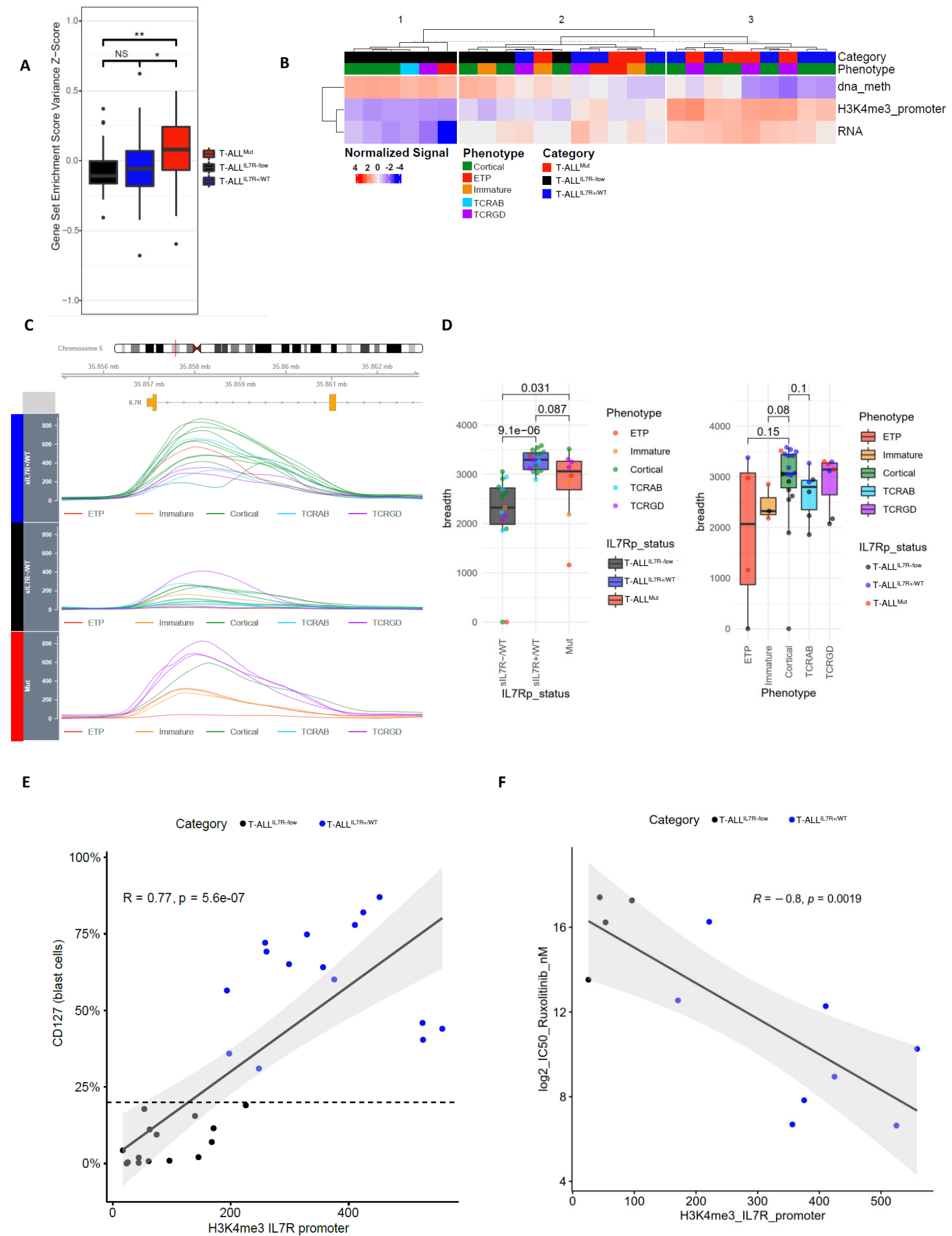
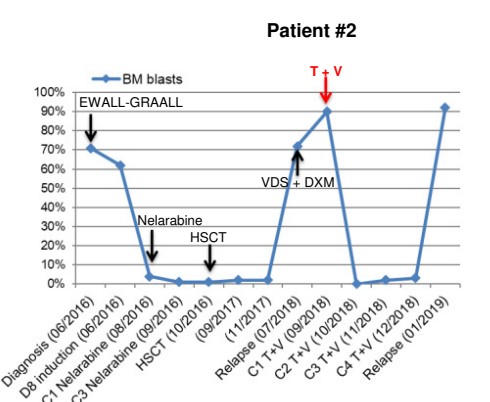
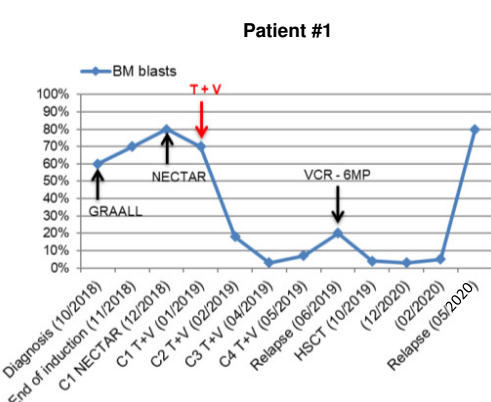
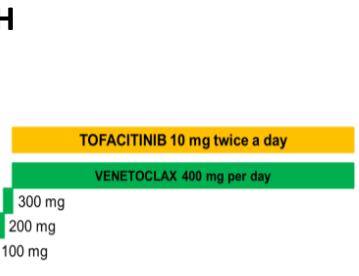
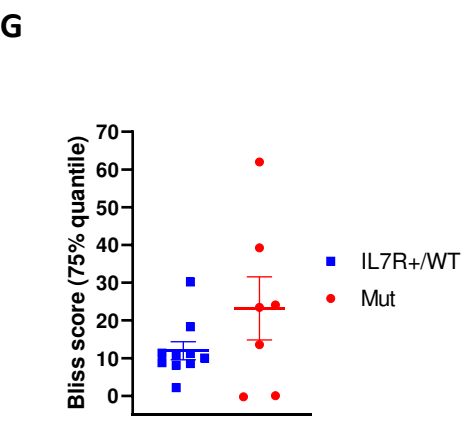
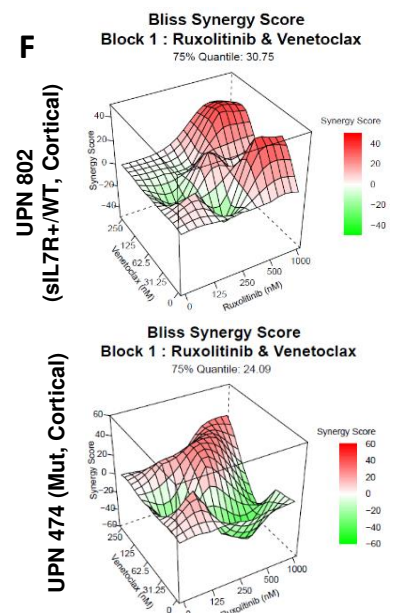
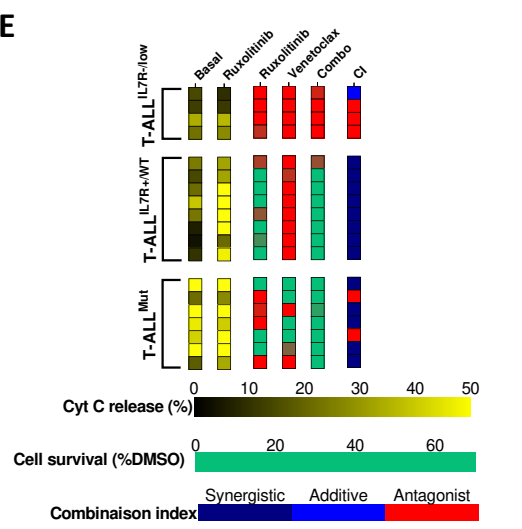
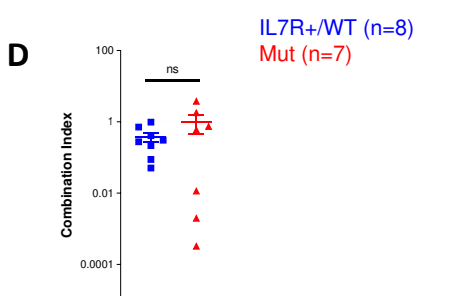
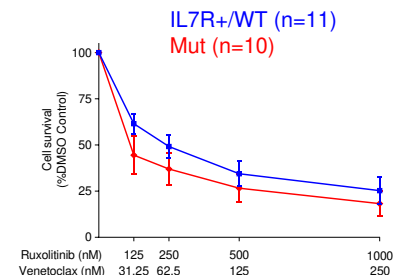
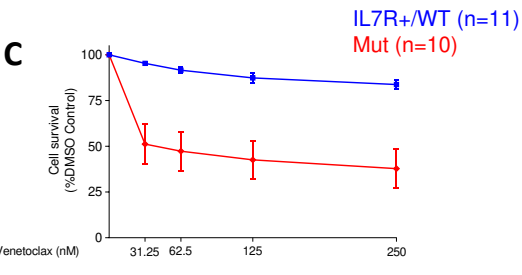
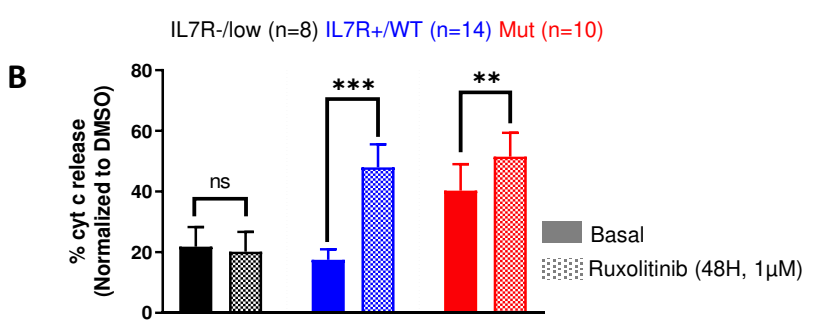
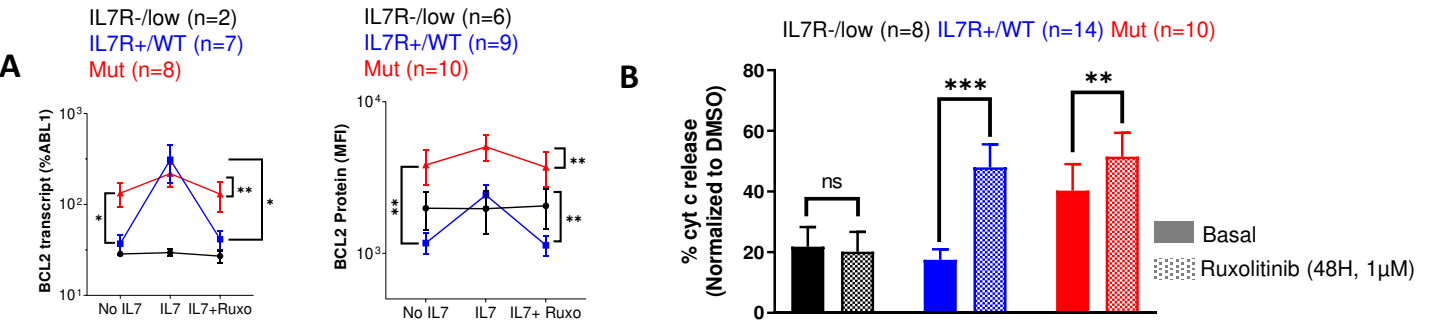




**Figure 6. BCL-2 and JAK-1 cotargeting is synergistic in CD127+ T-ALL, irrespective of IL7R $\beta$  mutational status**



## Title

**IL7-receptor expression is frequent in T-cell acute lymphoblastic leukemia and predicts sensitivity to JAK-inhibition**

## Running title

**IL7R-expressing T-ALL respond to JAK-inhibition**

## Authors:

Lucien Courtois<sup>1,2,3\*</sup>, Aurélie Cabannes-Hamy<sup>4\*</sup>, Rathana Kim<sup>5\*</sup>, Marine Delecourt<sup>2\*</sup>, Antoine Pinton<sup>1,2,3</sup>, Guillaume Charbonnier<sup>1,6</sup>, Mélanie Feroul<sup>2</sup>, Charlotte Smith<sup>1,2,3</sup>, Giulia Tueur<sup>2</sup>, Cécile Pivert<sup>2</sup>, Estelle Balducci<sup>1,2,3</sup>, Mathieu Simonin<sup>1,2,3</sup>, Laure Hélène Angel<sup>2</sup>, Salvatore Spicuglia<sup>6</sup>, Nicolas Boissel<sup>5</sup>, Guillaume P. Andrieu<sup>1</sup>, Vahid Asnafi<sup>1,2,3</sup>, Philippe Rousselot<sup>4</sup>, Ludovic Lhermitte<sup>1,2,3</sup>.

**Correspondence to:** [ludovic.lhermitte@aphp.fr](mailto:ludovic.lhermitte@aphp.fr)

## Affiliations :

<sup>1</sup> Université Paris Cité, INSERM UMR-S1151, CNRS UMR-S8253, Institut Necker Enfants Malades, F-75015 Paris, France.

<sup>2</sup> Hôpital Necker Enfants-Malades, Laboratoire d'Onco-Hématologie, Assistance Publique-Hôpitaux de Paris (AP-HP), Paris, France.

<sup>3</sup> Université Paris Cité, Paris, France.

<sup>4</sup> Department of Hematology and Oncology, Centre Hospitalier de Versailles, Le Chesnay, France.

<sup>5</sup> Université Paris Diderot, Institut Universitaire d'Hématologie, EA-3518, Assistance Publique-Hôpitaux de Paris, University Hospital Saint-Louis, Paris, France.

<sup>6</sup> Aix-Marseille University, Theories and Approaches of Genomic Complexity (TAGC), INSERM Unité Mixte de Recherche (UMR)1090 13288 Marseille, France.

\* These authors equally contributed to this work

### **Data Sharing Statement**

Accession numbers:

Study : EGAS00001007144 (<https://ega-archive.org/studies/EGAS00001007144>)

Dataset : EGAD00001010273

### **Key points**

- **IL7R/CD127 expression is frequent in T-ALL (~70%) and aberrantly diverges from normal thymocytic development**
- **IL7R/CD127 expression predicts sensitivity to JAK-inhibition in T-ALL and synergism with BCL2-inhibition**

## Abstract

T-cell acute lymphoblastic leukemia (T-ALL) is an aggressive hematological malignancy with a dismal prognosis related to refractory/relapsing diseases, raising the need for new targeted-therapies. Activating mutations of the IL7-receptor pathway genes (IL7Rp) play a proven leukemia-supportive role in T-ALL. JAK-inhibitors such as ruxolitinib have recently demonstrated preclinical efficacy. However, prediction markers for sensitivity to JAK-inhibitors are still lacking. Herein, we show that IL7R (CD127) expression is more frequent (~70%) than IL7Rp-mutations in T-ALL (~30%). We compared the so-called non-expressers (no IL7R-expression/IL7Rp-mutation), expressers (IL7R-expression without IL7Rp-mutation) and mutants (IL7Rp-mutations). Integrative multi-omics analysis outlined IL7R-deregulation in virtually all T-ALL subtypes, at the epigenetic-level in non-expressers, genetic-level in mutants, and post-transcriptional level in expressers. Ex-vivo data using primary-derived xenografts support that IL7Rp is functional whenever the IL7R is expressed, regardless of the IL7Rp mutational status. Consequently, ruxolitinib impaired T-ALL survival in both expressers and mutants. Interestingly, we show that expressers displayed ectopic IL7R-expression and IL7Rp-addiction conferring a deeper sensitivity to ruxolitinib. Conversely, mutants were more sensitive to venetoclax than expressers. Overall, combination of ruxolitinib and venetoclax resulted in synergistic effects in both groups. We illustrate the clinical relevance of this association by reporting achievement of complete remission in two patients with refractory/relapsed-T-ALL. This provides proof of concept for translation of this strategy into clinics as bridge to transplant. Altogether, IL7R-expression can be used as a biomarker for sensitivity to JAK-inhibition, thereby expanding the fraction of T-ALL patients eligible to ruxolitinib up to nearly ~70% of T-ALL.

## Introduction

T-ALL is a heterogeneous disease that results from malignant proliferation of immature T-cells blocked at varying stages of differentiation, which partially recapitulate normal lymphoid T-cell ontogeny.<sup>1</sup> The development of intensive chemotherapy regimens has considerably improved the outcome of adult T-ALL. Yet, relapsed disease conveys a dismal prognosis with a 6-to-9 months median survival.<sup>2-5</sup> Therefore, it remains an essential clinical challenge with urgent needs to identify relevant druggable targets and develop new therapeutic approaches for refractory/relapsed T-ALL patients.

IL7-receptor pathway (IL7Rp) plays a key role in normal T-cell development.<sup>6,7</sup> Binding of IL7 to IL7R initiates the formation of a trimeric complex between the cytokine, IL7R $\alpha$  specific chain (CD127 or IL7R) and the common  $\gamma$ -chain, leading to Janus kinases 1 (JAK1) and 3 (JAK3) transphosphorylation.<sup>8,9</sup> Subsequent phosphorylation of tyrosine residues in the cytoplasmic tail of CD127/IL7R $\alpha$  creates docking sites for effector molecules, notably signal transducer and activator of transcription 5 (STAT5) and phosphatidylinositol 4,5-bisphosphate 3-kinase (PI3K).<sup>10</sup> Phosphorylated STAT5 translocates into the nucleus, where it regulates proliferation and cell survival through transcriptional regulation of p27<sup>kip1</sup> and B-cell lymphoma 2 (BCL2).<sup>11,12</sup>

Somatic gain-of-function (GOF) mutations in IL7R $\alpha$  or downstream effectors (JAK1, JAK3, STAT5B) have been reported in up to ~30% of pediatric<sup>13</sup> and adult<sup>14</sup> T-ALL promoting cell transformation *in vitro* and tumor formation *in vivo*.<sup>15,16</sup> IL7Rp signaling negatively regulates *in vitro* steroid/chemo-sensitivity in childhood T-ALL by rescuing leukemic cells from mitochondrial-induced apoptosis, suggesting an important role of

BCL2-family of proteins.<sup>17–19</sup> Hence, IL7Rp represents a relevant druggable target, notably since clinically approved pharmacological inhibitors exist, such as JAK inhibitors (JAKinibs), including ruxolitinib (JAK1/2), and tofacitinib (JAK3). A seminal study demonstrated that ruxolitinib could delay disease progression *in vivo* in Early T-cell Progenitor (ETP) ALL, a subcategory of immature T-ALL characterized by a high incidence of IL7Rp mutations.<sup>20,21</sup> Consistent with this, treatment with ruxolitinib sensitizes the leukemia cells to glucocorticoids.<sup>18</sup> Another study evidenced the oncogenic role of IL7R per se in a IL7R-overexpressing murine model that could represent a relevant target.<sup>22</sup> Moreover, recent reports suggested the targeting of BCL2 as an efficient strategy in ETP-ALL and identified specific phosphoproteomic signatures that could predict synergism between JAK3 inhibitors and BCL2 inhibitors such as venetoclax.<sup>23–25</sup> This raised for the first time the utility of dual inhibition of the JAK and BCL2 molecules in T-ALL.

Although there is a strong rationale for the use of JAK inhibitors in IL7Rp-mutated ETP-ALL, whether this drug could benefit other T-ALL subtypes remains under debate.<sup>20,22,26</sup> In this study, we interrogated the IL7R pathway in T-ALL using a multi-level integrated approach to identify patients eligible to JAK-inhibition. We found that IL7R ectopic expression is a frequent oncogenic driver in T-ALL irrespective of the IL7Rp-mutational status, and predicts sensitivity to ruxolitinib. Finally, combination of venetoclax led to synergistic effects in IL7R-expressing T-ALL regardless of the IL7Rp-mutational status.

## Methods

### Patients and primary samples

Bone marrow or blood patient samples were collected after informed consent was obtained at diagnosis, in accordance with the Declaration of Helsinki and institutional guidelines. Mononuclear cells were isolated by ficoll density gradient prior to DNA extraction and cryopreservation. Immunophenotypic and molecular characterization of T-ALL samples were performed as previously described.<sup>27–29</sup>

### Thymic subpopulations sorting

Human thymic subpopulations were obtained from children undergoing cardiac surgery. Informed consent was obtained from parents and the study was approved by the Ethics committee (CPP Ile-de-France, project-number 2012-03-04). Cell-sorting of thymocytes was performed as previously described.<sup>30,31</sup>

### PDX generation

Patient-derived xenografts (PDX) were generated from primary T-ALL samples as previously reported.<sup>32</sup> Briefly,  $10^6$  viable leukemic cells were xenografted by intravenous retro-orbital injection in 6-weeks old NSG-mice. Mice were monitored weekly by flow cytometry for leukemic load (FSC<sup>hi</sup>/hCD7+/hCD45+ cells) in peripheral blood. Animals were clinically and biologically monitored until endpoint was reached or terminally ill, according to local ethical rules and home office license (30078-2021021814199445). Bone marrow from tibiae/hip/femora/vertebrae was collected for subsequent *ex vivo* experiments. All samples used contained  $\geq 90\%$  blasts.

## **Drug testing and flow cytometric experiments**

PDX were cultured in complete medium, supplemented with 50 ng/ml human stem cell factor, 20 ng/ml hFLT3-L, 10 ng/ml hIL7 and 20 nM insulin (Miltenyi-Biotec, Bergisch Gladbach, Germany). Cultures were maintained at 37°C in a humidified atmosphere containing 5% CO<sub>2</sub>. PDX cells were incubated with increasing doses of Ruxolitinib and/or Venetoclax for 96h. Cell viability and proliferation were determined by flow cytometry (FC) by Annexin-V-APC/propidium-iodide co-staining (BD-Pharmingen, San Jose, CA, USA) and CellTrace™ Violet Cell Proliferation Kit (ThermoFisher, Waltham, MA) respectively, according to manufacturer's instructions. CD127 expression was evaluated by FC using a mouse anti-human CD127 BV421-conjugated antibody (clone HIL7R-M21 (RUO)) (BD Biosciences, San Francisco, CA, USA). CD127 was considered positive whenever the percentage of positive cells was ≥20%. The gating strategy is described in the Supplemental Methods, as well as phosphoflow analyses. Cytochrome c-release experiments were performed as previously described<sup>33</sup>. Data were analyzed using DIVA/FlowJo softwares (BD Biosciences).

## **Molecular analyses**

Molecular experiments are described in the Supplemental Method section.

## **Statistical analyses**

Statistical analyses were performed using GraphPad Prism 8 software (GraphPad Software, San Diego, CA, United States) and R. Normality tests were applied to determine if the datasets were eligible to either parametric or non-parametric tests. Combination indexes (CI) were computed using the CompuSyn software and the Chou-Talalay method.<sup>34</sup> Bliss-scores were computed using the online-software synergyfinder.<sup>35</sup>





## Results

### **CD127 expression is regulated post-transcriptionally during human thymopoiesis**

We first evaluated the expression of IL7R/CD127 during normal early T-cell development by flow cytometry (FC). CD127 was expressed in the immature CD4/8-double-negative (DN) thymocytic stage, and was then progressively and dramatically repressed during the cortical stage in CD4/8-double-positive (DP) cells, consistent with IL7R signaling downregulation during  $\beta$ -selection.<sup>36–38</sup> Finally, expression reappeared at the ultimate maturation stage in CD4 and CD8 single-positive cells (SP4, SP8) (Figure 1A). We then measured transcriptional expression of *IL7R* over T-cell differentiation in electronically sorted thymic subpopulations. By contrast, *IL7R* transcriptional expression, as assessed by qRT-PCR and bulk RNA-seq, did not show significant differences across the thymocyte differentiation stages (Figure 1B). Similarly, analysis of RNA-seq data from a recent work on sorted thymocytes showed little variation of IL7R expression across T-cell differentiation (Supplemental Figure 1).<sup>39</sup> Altogether, these results suggest that IL7R expression is regulated at a post-transcriptional level during thymopoiesis.

### **CD127 expression is frequent and follows an aberrant pattern in T-ALL**

*IL7R* transcript expression remained stable, on average, across differentiation stages of T-ALL just like normal thymocytes (Figure 1C). Only ETP-ALL showed lower *IL7R* transcript. This finding was confirmed in two publicly available datasets (Supplemental Figure 2).<sup>21,40</sup> To the best of our knowledge, very limited data is currently available concerning the protein expression of CD127 in T-ALL.<sup>41–43</sup> We thus prospectively evaluated CD127 expression by FC in a large cohort of 200 primary diagnostic samples of adult T-ALL. Overall, CD127 was widely expressed in this series (70%) (Figure 1D), and found in every immunophenotypic subtype of T-ALL (Figure 1E, Supplemental Figure 3). Interestingly, the vast majority of cortical T-ALL cases (81%) expressed CD127, in sharp contrast with their physiological counterpart (Figure 1E). Conversely, CD127 expression was minimal in ETP-ALL and mature TCR $\alpha\beta$  T-ALL, again contrasting with the physiological pattern of normal thymocytes that normally express the receptor at these differentiation stages. (Figures 1 A,E). We found a similar expression (68%,  $p=ns$ ) in a retrospective analysis of 100 pediatric T-ALL (Figure 1D). Altogether, we evidenced an aberrant pattern of CD127 expression as regard to their physiological counterpart in T-ALL.

### **CD127 expression and IL7Rp mutational status define 3 groups of T-ALL**

We then analyzed the mutational status of the IL7Rp-genes (IL7R/JAK1/JAK3/STAT5B) in the 200 T-ALL adult cases. We found that 35% of these cases harbored at least one IL7Rp GOF mutation (Supplemental Figure 4). As we found far less IL7Rp mutations (~35%) than CD127 expression (~70%) in adult T-ALL, we integrated data from both mutational status and CD127 expression and identified 3 categories of T-ALL: non-expressers, with neither detectable CD127 expression nor IL7Rp mutation (T-ALL<sup>IL7R-/low</sup>); expressers, with CD127 expression without IL7Rp mutation (T-ALL<sup>IL7R+/WT</sup>); and mutants with mutations within the IL7Rp (T-ALL<sup>Mut</sup>), which also usually expressed the CD127 in >80% of cases (Figure 2A).

Mutants mostly segregated with the ETP/immature and TCR $\gamma\delta$  T-ALL, as previously described.<sup>14</sup> Expressers were mostly represented by cortical T-ALL while non-expressers were enriched in TCR $\alpha\beta$  T-ALL (Figure 2B). Consistent with this, mutants were enriched in HOXA9 overexpression, while expressers frequently overexpressed TLX1/TLX3 and non-expressers displayed frequent SIL-TAL microdeletions (Figure 2C). We then compared the mutational landscape of the 3 groups. Overall, expressers and mutants were similar (Supplemental Figure 5). By contrast, the T-ALL<sup>IL7R-/low</sup> subset was enriched in PTEN alterations while NOTCH1 mutations were less frequent (Supplemental Figure 5). Of note, PHF6 alterations were less frequent in this subset, consistent with recent findings showing that PHF6 mutations cooperate with IL7R.<sup>44</sup>

We questioned the stability of both expression and mutational status from diagnosis to relapse. To address this, we sequenced paired samples from diagnosis and relapse in a unique dataset of 131 relapsing T-ALL. Overall, the IL7Rp mutational status was retained in 91% of cases at relapse. Interestingly, integrative analysis of

both IL7Rp mutational status and CD27 expression revealed that CD127 expression was retained in 95% of cases (Supplemental Figure 6).

## **JAK1 inhibition abrogates IL7-induced JAK/STAT-signaling in CD127-expressing T-ALL, irrespective of IL7Rp mutational status**

To gain insight into signaling functionality of IL7Rp at a high resolution, we first evaluated the capacity of normal thymocytes to respond to IL7 stimulation by measuring STAT5 Y694 phosphorylation (pSTAT5) as a readout for IL7R signaling activation (Figure 3A). Immature and mature thymocytes but not cortical thymocytes did phosphorylate STAT5 in response to IL7. Consequently, CD127 expression and functional activation were closely related showing that, whenever the receptor is expressed, it is functional in normal thymocytes. Furthermore, IL7-induced STAT5 activation was fully abrogated in every thymocytic subset after exposure to ruxolitinib, a JAK1/2 inhibitor (Figure 3A).

We sought to determine whether this relation was preserved in the context of T-ALL. To address this, we generated 46 PDX from mutants, expressers and non-expressers (Figure 3B, Supplemental Figure 7). Overall, PDX recapitulated CD127 expression and IL7Rp mutational pattern of the primary diagnostic T-ALL samples, thus confirming PDX as a relevant model of the biology of the primary tumor (Supplemental Tables 1-4).

As expected, non-expressers had no constitutive phosphorylation of STAT5 at basal state, nor did they respond to IL7 stimulation (Figure 3C, Supplemental Figure 8). This was further supported by the absence of variation of transcriptional expression of the STAT5 targets *CISH* and *PIM1* in response to IL7 or IL7+ruxolitinib (Figure 3D). Conversely, mutants showed constitutive phosphorylation of STAT5 ( $p < 0.001$ , Mann-Whitney test) which was magnified in response to IL7, consistent with the transcriptional increase of *CISH* and *PIM1*. Interestingly, STAT5 phosphorylation was reversed with ruxolitinib exposure supporting that constitutive

pSTAT5 signaling is JAK1-dependent and that ruxolitinib abrogates inducible and partially constitutive IL7R signaling bringing back pSTAT5 levels close to baseline. Noteworthy, pSTAT5 was also abrogated in two T-ALL with STAT5B mutation (Supplemental Table 2, data not shown). Finally, expressers did not show any constitutive STAT5 activation as expected, but they still did respond to IL7 ligand to similar level as mutants, supporting functional IL7-dependent IL7R signaling.<sup>45</sup> Inducible activation could be fully reversed by ruxolitinib and kinetics of *CISH* and *PIM1* transcripts followed STAT5 phosphorylation. Altogether, CD127 expression predicted functional signaling of IL7Rp in T-ALL as in normal T-cell counterpart, and JAK1-inhibition was able to abrogate both constitutive and inducible IL7R-signaling.

## **Ruxolitinib efficacy depends on CD127-expression irrespective of the IL7Rp mutational status**

We then aimed to address whether JAK-inhibition by ruxolitinib could significantly impact cell survival and proliferation. Ruxolitinib had no impact on cell survival in non-expressers, as expected. Interestingly, exposure to ruxolitinib resulted in significant apoptosis in both mutants and expressers, with an even deeper sensitivity to ruxolitinib of expressers over mutants ( $p=0.0102$  for 500nM, Mann-Whitney test) (Figure 4A). It is well established that ruxolitinib sensitivity is linked to IL7-dependent viability<sup>46</sup>. As we cultured PDX T-ALL cells with supra-physiological IL7 concentrations (10ng/mL), this raised the question as to whether ruxolitinib efficacy could be influenced by local IL7 concentrations. We show in 4 PDX from expressers that cell survival was dramatically impaired upon ruxolitinib irrespective of the ambient IL7 concentration (Figure 4B). We then evaluated cell proliferation in fresh ex-vivo cultured PDX cells (Figure 4C-D). As expected, non-expressers were neither affected by IL7 stimulation nor ruxolitinib exposure. Conversely, cell proliferation dramatically decreased in both mutants and expressers (Figure 4C-D, Supplemental Figure 9) supporting cytostatic effects of ruxolitinib in all but non-expressers. Of interest, cytostatic effects were still observed in T-ALL cases with mild ruxolitinib-induced cytotoxicity (Supplemental Figure 9C-D). Overall, our data support that sensitivity to ruxolitinib is not exclusive of mutants and reaches CD127-expressing T-ALL irrespective of their IL7Rp mutational status.



## **T-ALL<sup>IL7R+/WT</sup> highly sensitive to ruxolitinib are characterized by broad H3K4me3 domains on IL7R promoter**

We analyzed steady-state bulk RNA-seq data and observed an active IL7Rp transcriptional signature in mutants which was absent in expressers (Figure 5A). We only found higher *IL7R* and *Pim1* transcripts in expressers as compared to non-expressers, suggesting a priming of IL7Rp but no constitutive activation (Supplemental Figure 10). We thus asked whether expression and functionality of *IL7R* could be epigenetically dictated. To address this question, we examined *IL7R* using a multi-omic approach combining whole-CPG DNA methylation data, RNA-seq and H3K4me3 CHIP-seq data<sup>47</sup>. As expected, non-expressers were characterized by a strong level of DNA methylation, minimal IL7R transcript and H3K4me3 activating mark (cluster 1, Figure 5B and Supplemental Figure 10). Conversely, cluster 3 was characterized by minimal levels of IL7R DNA methylation, high levels of IL7R transcript and H3K4me3 mark, and comprised only IL7R-expressing cases. Cluster 2 displayed intermediate features mixing both IL7R expressing and non-expressing cases. Interestingly, the level of H3K4me3 mark on IL7R promoter appeared to best identify cluster 3. Therefore, we looked at this mark associated with transcriptional elongation on additional T-ALL primary samples. Strikingly, expressers were characterized by broad H3K4me3 domains, especially in cortical T-ALL. In contrast, non-expressers were characterized by sharp H3K4me3 domains (Figure 5C-D). We previously showed that H3K4me3 broad domains were present on IL7R promoter in thymocytes subpopulations, including at the cortical stage.<sup>48</sup> However, CD127 is physiologically downregulated and non-responsive at this stage (Figures 1A and 3A), while cortical T-ALL are often CD127+ and respond to stimulation (Figures 2B and 3C), suggesting the loss of a post-transcriptional mode of regulation in T-ALL. In line

with this hypothesis, CD127 expression and H3K4me3 breadth were correlated in T-ALL (Figure 5E). Finally, we asked whether this apparent ectopic expression could be associated with an oncogenic addiction to IL-7. In line with this, we found that IC50 for ruxolitinib was inversely correlated with H3K4me3 signal (Figure 5F). Altogether, our data support ectopic expression and oncogenic IL7-addiction in cortical T-ALL which can be reversed by JAK-inhibition.

## **Cotargeting of BCL2 and JAK1 is synergistic in CD127-expressing T-ALL irrespective of the IL7Rp mutational status**

The IL7Rp is known to promote T cell survival via induction of antiapoptotic proteins such as BCL-2.<sup>11</sup> Potent clinically-grade BCL2 inhibitors such as venetoclax have proven efficient in T-ALL.<sup>23,24</sup> Recent studies showed that JAK-inhibition combined with targeting of BCL2 results in synergistic effects on cells transformed with JAK3 or IL7R $\alpha$  mutants.<sup>25,49</sup> We hypothesized that this cotargeting may not only benefit to mutants but could also extend to expressers. To address this question, we performed a dynamic evaluation of BCL2 transcript and protein expression upon stimulated (IL7) and inhibited (IL7+Ruxolitinib) conditions. Mutants showed a constitutive IL7-independent overexpression of BCL2 transcript and protein which was weakly sensitive to IL7 stimulation and ruxolitinib (Figure 6A). Interestingly, JAK1 inhibition impaired IL7-induced BCL2 expression but not constitutive BCL2 overexpression. This contrasts with our previous observation that ruxolitinib abrogates inducible and partially constitutive pSTAT5 activation in mutants (Figure 3C). BCL-2 expression dramatically increased upon IL7 stimulation in expressers and ruxolitinib fully abrogated this IL7-inducible expression (Figure 6A).

Mitochondrial apoptosis results from complex interactions of proteins from the BCL2-family, and measurement of the sole protein levels may not reflect the dominant anti-apoptotic mechanism.<sup>50</sup> To properly assess the functional dependency to the BCL2 molecule, we measured cytochrome c release at basal state and after pre-exposition to ruxolitinib (priming) (Figure 6B). Our data showed that mutants displayed strong functional dependency to BCL2 which was not altered by JAK-inhibition. By contrast, expressers were poorly dependent on the BCL2 molecule, but priming by ruxolitinib dramatically enhanced functional dependency on BCL2.

Altogether, JAK1 inhibition does not alter BCL2 constitutive dependency in mutants but increases BCL2 dependency in expressers (Figure 6B).

To assess whether this could predict sensitivity to venetoclax, we performed *ex vivo* cytotoxic assays using ruxolitinib and/or venetoclax. PDX from mutants were highly sensitive to venetoclax alone, consistent with the immature maturation stage of arrest (Figure 6C).<sup>23,24</sup> By contrast, T-ALL<sup>IL7R+WT</sup> were poorly sensitive to venetoclax at basal state but combo of ruxolitinib and venetoclax overcame this relative low-sensitivity and induced dramatic cell-death, as predicted by cytochrome-release assays.

A recent work suggested synergism of BCL2 and JAK1 co-inhibition in T-ALL with IL7Rp-mutations.<sup>49</sup> We wondered whether synergism would extend to all IL7R-expressing T-ALL, including expressers. Combo of venetoclax and ruxolitinib resulted in synergistic effects in both mutants and expressers, as supported by low combination indexes and Bliss scores (Figure 6D-G). Consequently, co-targeting JAK1 and BCL2 is synergistic in CD127-expressing T-ALL irrespective of the IL7R-pathway mutational status.

## **Efficacy of JAK and BCL2 co-inhibition in T-ALL patients**

We sought to determine how our *in vitro* and *ex vivo* results could translate into clinics. We report two adult patients with chemo-refractory IL7Rp-mutated ETP-ALL who were treated with the combination of tofacitinib, a JAK3-inhibitor that gave similar results as ruxolitinib (Supplemental Figure 11), and venetoclax (Figure 6H, Supplemental Table 5).

Patient 1 (Pt.1) obtained a rapid response after the first cycle of combination therapy (C1, 18% blast cells versus 70% pre-treatment). Venetoclax could be increased up to 800mg/day and Pt.1 attained a complete response with incomplete hematological recovery (CRi) at the end of C2. Combination therapy was well tolerated, without notable adverse events. However, at the end of C3, 7% bone marrow (BM) blast cells were noted and Pt.1 presented an overt relapse 2 months after CRi. Treatment with vincristine and 6 mercapto-purine allowed him to proceed to allogeneic hematopoietic stem cell transplant (allo-HSCT). Unfortunately, he relapsed 7 months after, and subsequently died of disease. Pt. 2 achieved CR with MRD negativity after C1. However, late acute graft versus host disease with cytopenia and fever occurred during C2, and was resolved with corticosteroid therapy and 3 weeks of combination therapy discontinuation, after which venetoclax was resumed at 400 mg/day and tofacitinib at 5mg x2/day. CR was maintained 3 months, until the end of C4, after which Pt.2 presented an overt relapse and subsequently died of disease. Altogether, combination of JAK and BCL2 inhibition enables achievement of CR for a couple of months and may be considered as a bridge-to-transplant therapy.

## Discussion

IL7R protein expression strongly associates with signaling functionality in both normal and malignant contexts so that, whenever the IL7R is expressed, it is functional. IL7R expression is tightly regulated in normal thymopoiesis and we confirm at the single cell level a dramatic decrease in IL7R expression around  $\beta$ -selection in accordance with previous literature<sup>36–38</sup>. Epigenetic and transcriptional data show no significant variation across the thymocytic differentiation stages suggesting a post-transcriptional/translational mechanism for control of IL7R expression. Keeping with this, previous reports showed activating marks with H3K4me3 broad domains on IL7R promoter at any stage of thymocytic differentiation<sup>48</sup>, as well as the role of SOCS<sup>37,51</sup> and DNMT<sup>52</sup> proteins in the regulation of IL7R expression and signaling

IL7R expression pattern is strongly aberrant from normal in T-ALL. A significant fraction of TCR $\alpha\beta$  T-ALL do not express IL7R, in contrast with their physiological counterpart. This may be related to the enrichment of SIL-TAL microdeletions leading to a transcriptional repression of IL7R.<sup>53</sup> This is also consistent with frequent PTEN deletions. The biology of mature TCR $\alpha\beta$  T-ALL thus differs from other T-ALL, with a PI3K-AKT driven oncogenesis unrelated to the JAK-STAT pathway.<sup>53–55</sup> Keeping with this, non-expressers harbor sharp H3K4me3 marks on IL7R promoter, consistent with an epigenetic drift of activating marks from cell identity genes to oncogenes in T-ALL.<sup>48</sup> On the other hand, IL7R expression culminates in cortical T-ALL, contrasting with their normal counterpart. This strongly suggests an oncogenic loss of the post-transcriptional/translational mechanism of regulation allowing for the ectopic and oncogenic expression of IL7R in cortical T-ALL. Finally, non-cortical T-ALL showed the presence of IL7R consistent with their

ontogenic counterpart, with constitutive activation supported by activating mutation of the IL7Rp. Altogether, our data suggest a dysregulation affecting the IL7Rp in most T-ALL: at the epigenetic level in non-expressers, genetic level in mutants, and post-transcriptional level in expressers. Functionally, this is consistent with the creation of supportive IL7R-signaling with ectopic neo-expression of the receptor in cortical-expressers, a reinforcement of the IL7Rp-signaling in mutants, but also the extinction of the IL7R-signaling in non-expressers allowing a switch to PI3K-AKT dependency.

While GOF mutations of IL7Rp account for 30% of T-ALL,<sup>13,14</sup> we report that IL7R expression is far more frequent, accounting for ~70% of T-ALLs as previously anticipated.<sup>41</sup> Our signaling studies show that IL7Rp activation results from cell-extrinsic and cell-intrinsic effects in T-ALL, which interestingly can be reversed by ruxolitinib. As expected, only mutants demonstrate cell-intrinsic signaling, while both mutants and expressers are IL7-responsive, thus highlighting the oncogenic importance of cell-extrinsic cues.<sup>45</sup> The functional consequence of this is that all but non-expressers respond to JAK-inhibition irrespective of the IL7Rp mutational status, resulting in decreased cell-proliferation and cell-viability. Sensitivity of T-ALL to JAK-inhibition in the absence of IL7Rp mutation has previously been evoked<sup>20,26</sup> and recently illustrated in a murine transgenic model.<sup>22</sup> However, the clinical significance of this observation remains elusive. Here, we provide the first large scale study that fully confirms CD127 as a biomarker for sensitivity to JAK-inhibition. This extends the eligibility of T-ALL for ruxolitinib beyond previously reported mutants or ETP-ALL<sup>20,25</sup>. This is of strong clinical significance as this drug could benefit to ~70% rather than 30% of overall T-ALL as previously anticipated.

We also outline subtle differences in drug sensitivity between mutants and expressers, with an even deeper sensitivity to ruxolitinib in expressers as compared

to mutants. Our data suggest that the maturation stage of arrest may explain these differences. Expressers comprise a majority of cortical T-ALL with an ectopic IL7R driving strong oncogenic signals. Conversely, mutants were mostly non-cortical T-ALL, where IL7R expression is reminiscent of the ontogeny and IL7R signaling is oncogenically reinforced by IL7Rp-mutation so that IL7Rp-activation plays as an additional driver. We speculate that ruxolitinib has more cytotoxic effects in expressers because it tackles a major oncogenic signal in cortical T-ALL. Conversely, mutants bear high BCL2 expression level reminiscent of their normal counterpart. While ruxolitinib fully abrogates inducible and partially constitutive pSTAT5, it only hampers inducible BCL2-expression, indicating a JAK-STAT-independent BCL2-expression in this context as previously suggested.<sup>56</sup> In contrast, expressers, enriched in cortical T-ALL, bear IL7-inducible and ectopic expression of BCL2 that is fully JAK-STAT dependent and reversed by ruxolitinib in this context. Importantly, addition of venetoclax results in a synergistic effect in both mutants and expressers. While venetoclax inhibits residual BCL2 in mutants, ruxolitinib polarizes apoptotic dependency to BCL2 in expressers.

Our data show that expression matters for selection of patients able to respond to the ruxolitinib+venetoclax combo. Flow-cytometric assessment of CD127 expression appears as a fast, easy and cheap companion test that is broadly applicable to screen patients for drug sensitivity. The evaluation of pSTAT5 Y694 could be considered as a more relevant functional readout. However, phospho-flow requires a dynamic test with in vitro IL7-stimulation, and it is far more challenging to standardize within diagnostic labs. We thus propose flow-cytometric assessment of CD127 expression as the best compromise in terms of applicability and clinical relevance to identify patients eligible for targeted therapy.



Altogether, this study provides valuable information to optimize translation of ruxolitinib and venetoclax to clinics for T-ALL patients with relapse who need therapeutics to bridge to transplant. This treatment protocol may benefit to a larger group of patients who may be selected with an easily applicable flow-cytometry-based companion test.

## References

1. Belver L, Ferrando A. The genetics and mechanisms of T cell acute lymphoblastic leukaemia. *Nat Rev Cancer*. 2016;16(8):494–507.
2. Gökbuget N, Kneba M, Raff T, et al. Adult patients with acute lymphoblastic leukemia and molecular failure display a poor prognosis and are candidates for stem cell transplantation and targeted therapies. *Blood*. 2012;120(9):1868–1876.
3. Desjonquères A, Chevallier P, Thomas X, et al. Acute lymphoblastic leukemia relapsing after first-line pediatric-inspired therapy: a retrospective GRAALL study. *Blood Cancer Journal*. 2016;6(12):e504–e504.
4. Gökbuget N, Stanze D, Beck J, et al. Outcome of relapsed adult lymphoblastic leukemia depends on response to salvage chemotherapy, prognostic factors, and performance of stem cell transplantation. *Blood*. 2012;120(10):2032–2041.
5. Litzow MR, Ferrando AA. How I treat T-cell acute lymphoblastic leukemia in adults. *Blood*. 2015;126(7):833–841.
6. Puel A, Ziegler SF, Buckley RH, Leonard WJ. Defective IL7R expression in T(-)B(+)NK(+) severe combined immunodeficiency. *Nat Genet*. 1998;20(4):394–397.
7. Barata JT, Durum SK, Seddon B. Flip the coin: IL-7 and IL-7R in health and disease. *Nat Immunol*. 2019;20(12):1584–1593.
8. Gonnord P, Angermann BR, Sadtler K, et al. A hierarchy of affinities between cytokine receptors and the common gamma chain leads to pathway cross-talk. *Sci Signal*. 2018;11(524):eaal1253.
9. McElroy CA, Holland PJ, Zhao P, et al. Structural reorganization of the interleukin-7 signaling complex. *PNAS*. 2012;109(7):2503–2508.
10. Ribeiro D, Melão A, Barata JT. IL-7R-mediated signaling in T-cell acute lymphoblastic leukemia. *Adv Biol Regul*. 2013;53(2):211–222.
11. Mazzucchelli R, Durum SK. Interleukin-7 receptor expression: intelligent design. *Nat Rev Immunol*. 2007;7(2):144–154.
12. Mackall CL, Fry TJ, Gress RE. Harnessing the biology of IL-7 for therapeutic application. *Nat Rev Immunol*. 2011;11(5):330–342.
13. Vicente C, Schwab C, Broux M, et al. Targeted sequencing identifies associations between IL7R-JAK mutations and epigenetic modulators in T-cell acute lymphoblastic leukemia. *Haematologica*. 2015;100(10):1301–1310.
14. Kim R, Boissel N, Touzart A, et al. Adult T-cell acute lymphoblastic leukemias with IL7R pathway mutations are slow-responders who do not benefit from allogeneic stem-cell transplantation. *Leukemia*. 2020;34(7):1730–1740.
15. Girardi T, Vicente C, Cools J, De Keersmaecker K. The genetics and molecular biology of T-ALL. *Blood*. 2017;129(9):1113–1123.

16. Oliveira ML, Veloso A, Garcia EG, et al. Mutant IL7R collaborates with MYC to induce T-cell acute lymphoblastic leukemia. *Leukemia*. 2022;36(6):1533–1540.
17. Wuchter C, Ruppert V, Schrappe M, et al. In vitro susceptibility to dexamethasone- and doxorubicin-induced apoptotic cell death in context of maturation stage, responsiveness to interleukin 7, and early cyto-reduction in vivo in childhood T-cell acute lymphoblastic leukemia. *Blood*. 2002;99(11):4109–4115.
18. Delgado-Martin C, Meyer LK, Huang BJ, et al. JAK/STAT pathway inhibition overcomes IL7-induced glucocorticoid resistance in a subset of human T-cell acute lymphoblastic leukemias. *Leukemia*. 2017;31(12):2568–2576.
19. Meyer LK, Huang BJ, Delgado-Martin C, et al. Glucocorticoids paradoxically facilitate steroid resistance in T cell acute lymphoblastic leukemias and thymocytes. *J Clin Invest*. 2020;130(2):863–876.
20. Maude SL, Dolai S, Delgado-Martin C, et al. Efficacy of JAK/STAT pathway inhibition in murine xenograft models of early T-cell precursor (ETP) acute lymphoblastic leukemia. *Blood*. 2015;125(11):1759–1767.
21. Zhang J, Ding L, Holmfeldt L, et al. The genetic basis of early T-cell precursor acute lymphoblastic leukaemia. *Nature*. 2012;481(7380):157–163.
22. Silva A, Almeida ARM, Cachucho A, et al. Overexpression of wild-type IL-7R $\alpha$  promotes T-cell acute lymphoblastic leukemia/lymphoma. *Blood*. 2021;138(12):1040–1052.
23. Chonghaile TN, Roderick JE, Glenfield C, et al. Maturation Stage of T-cell Acute Lymphoblastic Leukemia Determines BCL-2 versus BCL-XL Dependence and Sensitivity to ABT-199. *Cancer Discovery*. 2014;4(9):1074–1087.
24. Peirs S, Matthijssens F, Goossens S, et al. ABT-199 mediated inhibition of BCL-2 as a novel therapeutic strategy in T-cell acute lymphoblastic leukemia. *Blood*. 2014;124(25):3738–3747.
25. Degryse S, de Bock CE, Demeyer S, et al. Mutant JAK3 phosphoproteomic profiling predicts synergism between JAK3 inhibitors and MEK/BCL2 inhibitors for the treatment of T-cell acute lymphoblastic leukemia. *Leukemia*. 2018;32(3):788–800.
26. Delgado-Martin C, Meyer LK, Huang BJ, et al. JAK/STAT pathway inhibition overcomes IL7-induced glucocorticoid resistance in a subset of human T-cell acute lymphoblastic leukemias. *Leukemia*. 2017;31(12):2568–2576.
27. Asnafi V, Beldjord K, Boulanger E, et al. Analysis of TCR, pT alpha, and RAG-1 in T-acute lymphoblastic leukemias improves understanding of early human T-lymphoid lineage commitment. *Blood*. 2003;101(7):2693–2703.
28. Trinquand A, Tanguy-Schmidt A, Ben Abdelali R, et al. Toward a NOTCH1/FBXW7/RAS/PTEN-based oncogenetic risk classification of adult T-cell acute lymphoblastic leukemia: a Group for Research in Adult Acute Lymphoblastic Leukemia study. *J Clin Oncol*. 2013;31(34):4333–4342.
29. Bond J, Marchand T, Touzart A, et al. An early thymic precursor phenotype predicts outcome exclusively in HOXA-overexpressing adult T-cell acute lymphoblastic leukemia: a Group for Research in Adult Acute Lymphoblastic Leukemia study. *Haematologica*. 2016;101(6):732–740.
30. Lhermitte L, Ben Abdelali R, Villarèse P, et al. Receptor kinase profiles identify a rationale for multitarget kinase inhibition in immature T-ALL. *Leukemia*. 2013;27(2):305–314.
31. Cieslak A, Charbonnier G, Tesio M, et al. Blueprint of human thymopoiesis reveals molecular mechanisms of stage-specific TCR enhancer activation. *Journal of Experimental Medicine*. 2020;217(9):e20192360.

32. Trinquand A, Dos Santos NR, Tran Quang C, et al. Triggering the TCR Developmental Checkpoint Activates a Therapeutically Targetable Tumor Suppressive Pathway in T-cell Leukemia. *Cancer Discov.* 2016;6(9):972–985.
33. Ryan J, Montero J, Rocco J, Letai A. iBH3: simple, fixable BH3 profiling to determine apoptotic priming in primary tissue by flow cytometry. *Biol Chem.* 2016;397(7):671–678.
34. Chou TC, Talalay P. Quantitative analysis of dose-effect relationships: the combined effects of multiple drugs or enzyme inhibitors. *Adv Enzyme Regul.* 1984;22:27–55.
35. Bliss CI. THE CALCULATION OF MICROBIAL ASSAYS. *Bacteriol Rev.* 1956;20(4):243–258.
36. Van De Wiele CJ, Marino JH, Murray BW, et al. Thymocytes between the beta-selection and positive selection checkpoints are nonresponsive to IL-7 as assessed by STAT-5 phosphorylation. *J Immunol.* 2004;172(7):4235–4244.
37. Yu Q, Park J-H, Doan LL, et al. Cytokine signal transduction is suppressed in preselection double-positive thymocytes and restored by positive selection. *J Exp Med.* 2006;203(1):165–175.
38. Marino JH, Tan C, Taylor AA, et al. Differential IL-7 responses in developing human thymocytes. *Hum Immunol.* 2010;71(4):329–333.
39. Roels J, Van Hulle J, Lavaert M, et al. Transcriptional dynamics and epigenetic regulation of E and ID protein encoding genes during human T cell development. *Frontiers in Immunology.* 2022;13:.
40. Liu Y, Easton J, Shao Y, et al. The genomic landscape of pediatric and young adult T-lineage acute lymphoblastic leukemia. *Nat Genet.* 2017;49(8):1211–1218.
41. Karawajew L, Ruppert V, Wuchter C, et al. Inhibition of in vitro spontaneous apoptosis by IL-7 correlates with bcl-2 up-regulation, cortical/mature immunophenotype, and better early cytoreduction of childhood T-cell acute lymphoblastic leukemia. *Blood.* 2000;96(1):297–306.
42. Barata JT, Keenan TD, Silva A, et al. Common gamma chain-signaling cytokines promote proliferation of T-cell acute lymphoblastic leukemia. *Haematologica.* 2004;89(12):1459–1467.
43. Asnafi V, Beldjord K, Garand R, et al. IgH DJ rearrangements within T-ALL correlate with cCD79a expression, an immature/TCRgammadelta phenotype and absence of IL7Ralpha/CD127 expression. *Leukemia.* 2004;18(12):1997–2001.
44. Yuan S, Wang X, Hou S, et al. PHF6 and JAK3 mutations cooperate to drive T-cell acute lymphoblastic leukemia progression. *Leukemia.* 2022;36(2):370–382.
45. De Smedt R, Morscio J, Reunes L, et al. Targeting cytokine- and therapy-induced PIM1 activation in preclinical models of T-cell acute lymphoblastic leukemia and lymphoma. *Blood.* 2020;135(19):1685–1695.
46. van der Zwet JCG, Buijs-Gladdines JGCAM, Cordo' V, et al. MAPK-ERK is a central pathway in T-cell acute lymphoblastic leukemia that drives steroid resistance. *Leukemia.* 2021;
47. Touzart A, Mayakonda A, Smith C, et al. Epigenetic analysis of patients with T-ALL identifies poor outcomes and a hypomethylating agent-responsive subgroup. *Science Translational Medicine.* 2021;
48. Belhocine M, Simonin M, Abad Flores JD, et al. Dynamic of broad H3K4me3 domains uncover an epigenetic switch between cell identity and cancer-related genes. *Genome Res.* 2021;gr.266924.120.

49. Senkevitch E, Li W, Hixon JA, et al. Inhibiting Janus Kinase 1 and BCL-2 to treat T cell acute lymphoblastic leukemia with IL7-R $\alpha$  mutations. *Oncotarget*. 2018;9(32):22605–22617.
50. Certo M, Del Gaizo Moore V, Nishino M, et al. Mitochondria primed by death signals determine cellular addiction to antiapoptotic BCL-2 family members. *Cancer Cell*. 2006;9(5):351–365.
51. Sharma ND, Nickl CK, Kang H, et al. Epigenetic silencing of SOCS5 potentiates JAK-STAT signaling and progression of T-cell acute lymphoblastic leukemia. *Cancer Sci*. 2019;110(6):1931–1946.
52. Tremblay CS, Brown FC, Collett M, et al. Loss-of-function mutations of Dynamin 2 promote T-ALL by enhancing IL-7 signalling. *Leukemia*. 2016;30(10):1993–2001.
53. Bornschein S, Demeyer S, Stirparo R, et al. Defining the molecular basis of oncogenic cooperation between TAL1 expression and Pten deletion in T-ALL using a novel pro-T-cell model system. *Leukemia*. 2018;32(4):941–951.
54. Kuzilková D, Bugarin C, Rejlova K, et al. Either IL-7 activation of JAK-STAT or BEZ inhibition of PI3K-AKT-mTOR pathways dominates the single-cell phosphosignature of ex vivo treated pediatric T-cell acute lymphoblastic leukemia cells. *Haematologica*. 2021;107(6):1293–1310.
55. Mendes RD, Sarmiento LM, Canté-Barrett K, et al. PTEN microdeletions in T-cell acute lymphoblastic leukemia are caused by illegitimate RAG-mediated recombination events. *Blood*. 2014;124(4):567–578.
56. Ribeiro D, Melão A, van Boxtel R, et al. STAT5 is essential for IL-7–mediated viability, growth, and proliferation of T-cell acute lymphoblastic leukemia cells. *Blood Adv*. 2018;2(17):2199–2213.

## Authorship

All authors generated the data. LL, LC, RK, MD and VA collected, analyzed and managed the data. LL, LC and RK wrote the manuscript. GC, GA and AP performed bioinformatic analyses. NB, ACH and PR provided clinical data. LL designed the concept of the work and supervised analyses and writing.

## Acknowledgments

This work was supported by INCA PLBIO 2021-1-PL BIO-04, Ligue Contre le Cancer « Enfants et Cancers de 2021 », L'association pour la Recherche contre le Cancer ARC Labellisation « PGA\_RC 2020 ROUSSELOT », La Fédération Leucémie Espoir, Force Hémato, Association Laurette Fugain “ALF 2021/04”. LC was supported by a grant from Fondation pour la Recherche Médicale (FRM, Poste de thèse pour

internes et assistants FDM201906008584). The corresponding author thanks the EHA-ASH joint-effort as a translational Research Trainee in Hematology (TRTH).

### **Conflict of Interest**

The authors have no conflict of interest to declare.

## Figure legends

### Figure 1: Landscape of IL7R expression in normal and malignant thymocytes

**A:** Surface IL-7R $\alpha$  chain (CD127 or sIL7R) expression was analysed by flow cytometry (FC) on gated thymocytic subpopulations from human thymi (n=3), as described in Methods. Left panel: a representative example is shown for a single thymus. Right panel: For each thymus, the median fluorescence intensity (MFI) of each thymocyte subpopulation was normalized to DP CD3<sup>+</sup> thymocytes MFI. The ratio of fluorescence intensity (RFI) is shown for each thymocytic subpopulation. Means and SEM are shown. DN: double negative, DP: double positive, ISP: immature simple positive, SP: single positive. **B:** Left panel: IL7R expression was analysed by RT-qPCR on thymocytic subpopulations sorted from 2 independent human thymi. *IL7R* transcript level is expressed as %ABL1 endogeneous control. Means and SEM are shown. Kruskal-Wallis test with post-hoc Dunn's multiple comparisons. Right panel: *IL7R* expression was assessed by bulk RNAseq on sorted thymic subpopulations from 1 human thymus. Normalized Log<sub>2</sub> expression values are shown. **C:** *IL7R* expression was analysed in a cohort of adult T-ALL cases by RT-QPCR (n=146) and bulk RNA-seq (n=156) as in (B). T-ALL were classified by immunophenotype. Means and SEM are shown. Kruskal-Wallis test with post-hoc Dunn's multiple comparisons. \*\*: p<0.01. **D:** CD127 (sIL7R) expression was assessed by flow cytometry in 200 adults and 100 pediatric unselected T-ALL cases. Bar graph depicts the proportion of sIL7R positive (orange) and negative (grey) cases in each group. Fisher's exact test. **E:** Left panel: sIL7R expression level (% of CD127 positive blasts) for each T-ALL from the adult cohort classified according to their immunophenotype (n=198). Means and SEM are shown. Kruskal-Wallis test with post-hoc Dunn's multiple comparisons. Right panel: Relative proportions of sIL7R+

and sIL7R-/low T-ALL from the adult cohort (n=198) for each immunophenotypic subgroup. The threshold of positivity was set at 20%. Chi-square test. \*\*\*\*: p<0.0001

### **Figure 2: CD127 expression and IL7Rp mutational status define 3 categories of T-ALL**

**A:** sIL7R expression level (% of CD127 positive blasts) for each T-ALL from the adult cohort (n=200) classified according to the combination of sIL7R status (positive if  $\geq 20\%$  blast cells) and IL7R/JAK1/JAK3/STAT5B mutational status in 3 categories (black, T-ALL<sup>IL7R-/low</sup> or non-expressers; blue, T-ALL<sup>IL7R+/WT</sup> or expressers, red, T-ALL<sup>Mut</sup> or mutants). **B:** Left panel: Bar chart depicts the relative proportions of the 3 T-ALL categories in each immunophenotypic subgroup (n=198). Chi-square test. \*\*\*\*: p<0.0001. Right panel: pie charts depict the relative proportions of the different immunophenotypic subgroups for the 3 T-ALL categories. **C:** Left panel: Bar chart depicts the relative proportions of the 3 T-ALL categories in each oncogenetic subgroup (n=190). Chi-square test. \*\*\*\*: p<0.0001. Right panel: pie charts depict the relative proportions of the different oncogenetic subgroups for the 3 T-ALL categories. None: overexpression of HOXA9, TLX1, TLX3 or SIL-TAL was not found.

### **Figure 3: Functional signaling and targeting of IL7Rp in normal and malignant thymocytes.**

**A:** Independent human thymi (n=2) were cultured for 15 minutes in complete medium deprived of IL-7 (basal state), supplemented with IL-7 (100ng/ml) (IL7), or supplemented with IL-7 and ruxolitinib (500nM) (IL7 + Ruxolitinib). pSTAT5 Y694 was then assessed by flow-cytometry for each condition and each subpopulation (histograms). Data are presented according to subsetting into thymocytic subpopulations. ISP: Immature Simple Positive, DN: Double-Negative, DP: Double-Positive, SP: Simple Positive. **B:** sIL7R expression (%CD127 positive blasts) on

Patient Derived Xenografts (PDX, n=46) used in the experiments. Samples are color-coded according to the category of the T-ALL from which they are derived. **C:** PDX cells were cultured as in **A** before being subjected to pSTAT5 Y694 analysis by flow-cytometry. Dot plots represent pSTAT5 Median of Fluorescence Intensity (MFI) for each case and each condition. Mean and SEM are represented. Friedman test with post-hoc Dunn's multiple comparisons. \*: p<0.05; \*\*: p<0.01; \*\*\*: p<0.001; \*\*\*\*: p<0.0001. **D:** PDX cells were cultured for 24 hours in complete medium deprived of IL-7, supplemented with IL-7 (100ng/ml), or supplemented with IL-7 and ruxolitinib (1 $\mu$ M) before RNA extraction and quantification of CISH (left panel) and PIM1 (right panel) by RT-qPCR. Mean and SEM are represented. Friedman test with post-hoc Dunn's multiple comparisons. Ns: not significant; \*: p<0.05; \*\*: p<0.01; \*\*\*: p<0.001; \*\*\*\*: p<0.0001.

**Figure 4: Ruxolitinib induces apoptosis and cytostatic effects in IL7R+ T-ALL, irrespective of the IL7R pathway mutational status.**

**A:** PDX cells were cultured for 96h in presence of rising concentrations of ruxolitinib. Cell viability was assessed at day 4 by FC (Annexin V/Propidium Iodide staining). Left panel: viability curves. Results are expressed as % cell survival normalized to a DMSO-treated condition (control). Right panel: histograms depict cell survival for each category in presence of ruxolitinib (1 $\mu$ M). Means and SEM are represented. Mann-Whitney test. \*: p<0.05; \*\*\*: p<0.001; \*\*\*\*: p<0.0001. **B:** PDX cells from 4 T-ALL<sup>IL7R+/WT</sup> were cultured in complete medium deprived of IL-7 (black) or supplemented with increasing concentrations of IL-7 (orange: 1ng/ml, red: 5ng/ml, brown: 10ng/ml). For each condition, cells were exposed to increasing concentrations of ruxolitinib and cell viability was assessed as in **A** after 72h of culture. Upper panel: bars depict raw viability (mean with SD) for control-treated conditions (DMSO). Lower



panel: Cell viability was normalized for each condition to the corresponding control-treated condition. Results are shown as mean with SD for each ruxolitinib concentration. **C**: PDX cells derived from 1 T-ALL<sup>IL7R-/low</sup>, 1 T-ALL<sup>Mut</sup> and 2 T-ALL<sup>IL7R+/WT</sup> were stained with CellTrace<sup>TM</sup> Violet cell proliferation kit and cultured in medium supplemented with IL-7 (black histograms), with IL-7 and ruxolitinib 1 $\mu$ M (red-filled histograms) or without IL-7 (violet-filled histograms). At day 7, cells were analyzed by FC to assess cell generations from living cells. **D**: Bar plot depicts the relative proportions of cell generations among living cells for 2 T-ALL<sup>IL7R-/low</sup>, 2 T-ALL<sup>Mut</sup> and 2 T-ALL<sup>IL7R+/WT</sup> following the same experimental procedure as in **C**. Note that the cell viability is affected by the absence of IL-7 or the presence of ruxolitinib in T-ALL<sup>Mut</sup> and T-ALL<sup>IL7R+/WT</sup> in contrast to T-ALL<sup>IL7R-/low</sup>.

**Figure 5: Expressers highly sensitive to ruxolitinib are characterized by broad H3K4me3 domains on IL7R promoter**

**A**: Gene set variation analysis (GSVA) between T-ALL<sup>IL7R-/low</sup> (n=26), T-ALL<sup>IL7R+/WT</sup> (n=28) and T-ALL<sup>Mut</sup> (n=42) using a custom IL-7R pathway gene set of 36 genes selected from reactome (REACTOME\_INTERLEUKIN\_7\_SIGNALING) and biocarta (BIOCARTA\_IL7\_PATHWAY) databases. Box plots show lower quartile, median and upper quartiles. Whiskers mark the 10<sup>th</sup> and 90<sup>th</sup> percentiles. Dots represent outliers. Kruskal-Wallis test with post-hoc Dunn's multiple comparisons test. NS: not significant, \*: p<0.05; \*\*: <0.01. **B**: *IL7R* was evaluated by a multi-omic approach combining EPIC-array, CHIP-seq and bulk RNA-seq on 10 T-ALL<sup>IL7R-/low</sup>, 9 T-ALL<sup>IL7R+/WT</sup> and 7 T-ALL<sup>Mut</sup>. The heatmap show the level of CpG-DNA methylation (dna\_meth), H3K4me3 breadth (H3K4me3\_promoter) on IL7R promoter/Transcription starting site (TSS) as well as IL7R transcript for each sample.

Samples are classified by k-means (k=3) then hierarchical clustering. For each metric, values were centered and reduced.

**C:** H3K4me3 tracks on IL7R promoter for 15 T-ALL<sup>IL7R+/WT</sup>, 8 T-ALL<sup>Mut</sup> and 15 T-ALL<sup>IL7R-/low</sup>. **D:** Box plots showing the breadth (bp) of H3K4me3 peaks on IL-7R TSS for the same T-ALL as in **C** according to the 3 categories defined in this article (left panel) or their phenotype (right panel). Mann-Whitney test. The *p*-value is indicated for each comparison. **E:** Correlation between sIL7R expression (% CD127-positive blasts) and H3K4me3 peak quantile-normalized coverage signal on IL7R promoter. The dashed line indicates the threshold for CD127 positivity (20%). Correlation curve and 95% Confidence Interval are shown. Pearson correlation test. **F:** Inverse correlation between ruxolitinib sensitivity (Log2 IC50) and H3K4me3 peak signal on IL7R promoter. Correlation curve and 95% Confidence Interval are shown. Pearson correlation test.

**Figure 6: BCL-2 and JAK-1 cotargeting is synergistic in CD127+ T-ALL, irrespective of IL7Rp mutational status**

**A:** PDX cells were cultured in complete medium deprived of IL-7 (No IL7), supplemented with IL-7 (100ng/ml) (IL7), or supplemented with IL-7 (100ng/ml) and ruxolitinib (1 $\mu$ M) (IL7+Ruxo). Bcl-2 expression was then analyzed for each condition by RT-qPCR after 24h of incubation (left panel: 2 T-ALL<sup>IL7R-/low</sup>, 7 T-ALL<sup>IL7R+/WT</sup> and 8 T-ALL<sup>Mut</sup>), and by flow cytometry after 48h of incubation (right panel: 6 T-ALL<sup>IL7R-/low</sup>, 9 T-ALL<sup>IL7R+/WT</sup> and 10 T-ALL<sup>Mut</sup>). Wilcoxon test for paired samples, Mann-Whitney test for unpaired samples. \*: *p*<0.05; \*\*: *p*<0.01. Means and SEM are represented. **B:** PDX cells from 8 T-ALL<sup>IL7R-/low</sup>, 14 T-ALL<sup>IL7R+/WT</sup> and 10 T-ALL<sup>Mut</sup> were cultured for 48h in complete medium alone (basal/static) or supplemented with ruxolitinib 1 $\mu$ M (dynamic). Cells were then exposed to venetoclax 1 $\mu$ M or DMSO for 1h before

cytochrome c release (cyt c release) assessment by flow cytometry. For each condition, results were obtained after venetoclax exposure and were normalized to the DMSO treated corresponding cells. Means and SEM are represented. DMSO (negative control) and alamethicin (positive control) were used to gate cytochrome c positive cells (see supplemental Methods). Ns: not significant, \*\*:  $p < 0.01$ ; \*\*\*:  $p < 0.001$ , Wilcoxon test. **C**: PDX cells from 11 T-ALL<sup>IL7R+/WT</sup> and 10 T-ALL<sup>Mut</sup> were cultured in presence of increasing concentrations of venetoclax alone (left panel) or in combination with ruxolitinib at a fixed ratio (ruxolitinib/venetoclax: 4/1, right panel). Cell viability was assessed after 96h of incubation by flow cytometry (Annexin V/PI staining). Results were normalized to a DMSO treated condition. Means and SEM are represented. **D**: Combination Indexes (CI) for the combination of ruxolitinib (1 $\mu$ M) and venetoclax (250nM) tested on 8 T-ALL<sup>IL7R+/WT</sup> and 7 T-ALL<sup>Mut</sup> as in **C**. CompuSyn software was used to calculate CI. A CI of 1 indicates an additive effect, CI < 1 a synergistic effect and CI > 1 antagonism. **E**: Heatmap summarizing datas presented in **B-D**. **F**: Representative 3D synergy plots of a T-ALL<sup>IL7R+/WT</sup> (upper panel) and a T-ALL<sup>Mut</sup> (lower panel) tested for the combination ruxolitinib and venetoclax. A Bliss score >10 indicates synergy, between -10 to 10: additivity, <-10: antagonism. The software Synergyfinder was used to draw synergy plots and calculate Bliss scores. **G**: Bliss score (75% quantile) for the combination ruxolitinib and venetoclax was calculated as in **F** for 10 T-ALL<sup>IL7R+/WT</sup> and 7 T-ALL<sup>Mut</sup>. **H**: Left panel: Treatment schedule for the combination of tofacitinib and venetoclax in patients with relapsed/refractory T-ALL. Middle panel: Bone marrow blast count evolution (% of mononuclear cells) in patient n°1. Therapeutic interventions are detailed above or below corresponding arrows. Right panel: Bone marrow blast count evolution (% of mononuclear cells) in patient n°2. Therapeutic interventions are detailed above or

below corresponding arrows. *BM: bone marrow; CX: cycle number X; D: Day; DXM: dexamethasone; EWALL: European Working Group on Adult ALL protocol; GRAALL: Group for Research on Adult Acute Lymphoblastic Leukemia protocol; HSCT: hematopoietic stem cell transplant; MRD: minimal residual disease; NECTAR : Nelarabine, cyclophosphamide, etoposide; T: Tofacitinib; V: Venetoclax; VCR: vincristine; VDS: vindesine; 6MP: 6-mercaptopurine*